ligand from one Mo–Ru edge to the second, is evident.[28]

Furthermore, the coalescence of the diastereotopic M–CO signals of the Cp* derivative **11** takes place at 303 K (Figure S3, supplementary material). At 345 K, the $^{13}C$ spectrum exhibits a very sharp Mo–CO signal and a less sharp Ru–CO signal, indicating that the intermetallic CO scrambling between the Mo and Ru atoms has not occurred. The kinetic barriers for the acetylide migration are summarized in Table IX.

**Factors That Affect the Site Selectivity and Barrier of the Acetylide Rotation.** The transition-metal atoms, the accessory ligand, and even the substituent on the acetylide ligand have considerable impact on both the location of the acetylide and the barrier of its fluxional behavior. In general, the acetylide C–C vector tends to interact more strongly with the M–M bond in the order

$$W\text{–}Os > Os\text{–}Os \qquad Mo\text{–}Ru \geq Ru\text{–}Ru \geq W\text{–}Ru$$

Furthermore, the barrier of the acetylide migration of the $WOs_2$ derivatives is clearly larger than those of the $WRu_2$ and $MoRu_2$ derivatives.

The electron-releasing and bulky substituents on the acetylide ligand and the more electron-releasing and bulky Cp* ligands on tungsten or molybdenum prefer the structure of symmetric isomer **b**. The dependence on the nature of the substituent R is indicated from the comparison of the **a**:**b** ratio of the pairs between **5** and **7**, **5** and **8**, **8** and **9**, **10** and **12**, and **11** and **13**, whereas the **a**:**b** ratio of the pairs between **4** and **5** and **12** and **13** accounts for the influence of the Cp* ligand (Table VIII). The origin of the electronic effect is uncertain at present. However, the steric effect is clearly due to the repulsion between the ligand L and the substituent R; the steric crowding between L and R of the symmetric isomer **b** is evidently smaller than that of the asymmetric isomer **a**.

The activation barrier of the acetylide migration shows values in the narrow range 61–72 kJ/mol (Table IX). From the variable-temperature NMR studies we conclude that the barriers for the rotation of the acetylide are much greater than those for the 3-fold localized rotation of the $CpW(CO)_2$, $CpMo(CO)_2$, and $Ru(CO)_3$ moieties in this system. The variation in these values also indicates that the barriers decreased when there is a better electron-releasing substituent R on acetylide or a better donor ligand Cp* on the transition-metal atom. This finding is in good agreement with our proposal that, in the transition state of the acetylide migration, the acetylide is perpendicular to the metal triangle; accordingly, the bonding interaction between the $\beta$-carbon and the metal atoms is weakened substantially. An electron-releasing substituent on the $\beta$-carbon and the Cp* ligand on the basal metal atom would definitely stabilize the transition state and decrease the barrier. This interpretation is valid even in the case in which the acetylide moiety adopts a tilted arrangement in the transition state ($\theta < 180°$).

**Acknowledgment.** We are grateful to the National Science Council of the Republic of China for financial support (Grant No. NSC79-2008-M007-52).

**Supplementary Material Available:** Three variable-temperature $^{13}C$ NMR spectra (Figures S1–S3) and tables of nonessential bond distances and angles and anisotropic thermal parameters for **1**, **4**, and **10** (12 pages); listings of the observed and calculated structural factors for **1**, **4**, and **10** (37 pages). Ordering information is given on any current masthead page.

# Bimetallic Macrocyclic Zirconocene Dialkoxides: Synthesis, Structure, Bonding, and Molecular Modeling Considerations

Douglas W. Stephan

*Department of Chemistry and Biochemistry, University of Windsor, Windsor, Ontario, Canada N9B 3P4*

*Received March 1, 1990*

The reactions of $Cp_2ZrMe_2$ with the diols 2,2-dimethylpropane-1,3-diol and 1,3-benzenedimethanol proceed with evolution of methane, affording the macrocyclic zirconocene dialkoxides $Cp_2Zr(\mu\text{-}OCH_2C(CH_3)_2CH_2O)_2ZrCp_2$ (**1**) and $Cp_2Zr(\mu\text{-}OCH_2C_6H_4CH_2O)_2ZrCp_2$ (**2**), respectively. Complex **1** crystallizes in the tetragonal space group $P4_2mnm$ with $a$ = 8.585 (2) Å, $c$ = 20.200 (2) Å, $Z$ = 2, and $V$ = 1448.7 (5) Å$^3$. Molecule **2** crystallizes in the trigonal space group $R\bar{3}$ with $a$ = 18.976 (4) Å, $Z$ = 3, and $V$ = 2485.6 (8) Å$^3$. In the case of **1**, a disorder in the structural data is consistent with two possible conformations of the 12-membered dimetalated ring. Molecular mechanics calculations in which the geometry at Zr is fixed were performed for the two possible conformers. The pseudocrown conformation is predicted to be thermodynamically more stable than the pseudochair form. In contrast, complex **2** adopts a pseudochair conformation. In addition, the disposition of the alkyl substituents on the oxygen atoms is endo for **1** and exo for **2**. These structural differences between **1** and **2** are considered and discussed. The nature of the Zr–O bonding in these complexes is discussed in terms of the extended Hückel molecular orbital picture. The structural and theoretical data support the notion of significant $\pi$-bonding between Zr and oxygen.

## Introduction

Early-metal oxides such as titania and zirconia are often employed as support materials for heterogeneous catalysts.[1] The support may act simply as a dispersent for the late-metal centers or may play an active role in the catalytic cycle. The latter instance gives rise to the phenomenon known as strong metal–support interactions (SMSI).[1] Cooperative activation of substrate molecules by a Lewis acidic early-metal center and a late-metal center has been proposed to account for this effect. Recent studies have investigated homogeneous systems in which early and late metals are linked in close proximity by bridging ligands.[2] Such heterobimetallics are of interest

(1) (a) *Metal-Support Interactions in Catalysis, Sintering, and Redispersion*; Stevenson, S. A., Dumesic, J. A., Baker, R. T. K., Ruckenstein, E., Eds.; Van Nostrand-Reinhold: New York, 1987. (b) *Strong Metal-Support Interactions*; Baker, R. T. K., Tauster, S. J., Dumesic, J. A., Eds.; American Chemical Society: Washington, DC, 1986.

0276-7333/90/2309-2718$02.50/0 

both as models for the heterogeneous catalyst systems and because of their potential as catalysts in their own right. Fewer studies have focused on simple complexes of Ti or Zr that might model the Lewis acidic early-metal centers of titania or zirconia. Recent works by several groups,[3-5] most notably that of Rothwell et al., have reported the syntheses and reaction chemistry of a variety of early-metal alkoxide complexes. The similarity of metal alkoxide species to metal oxides and the propriety of such species as models for metal oxide surfaces have been considered by others.[3] Work to date has largely involved the use of sterically demanding alkoxy or aryloxy ligands, which inhibit oligomerization and yield mononuclear early-metal compounds.[4,5] In initiating our investigations in this area, we describe the specific formation of bimetallic Zr alkoxide species via the reaction of dimethylzirconocene with simple diols. Structural and spectroscopic studies of these compounds are presented. The molecular geometries and the conformations of these macrocyclic complexes are considered by employing extended Hückel theory and molecular modeling techniques.

## Experimental Section

**General Data.** All preparations were done under an atmosphere of dry, $O_2$-free $N_2$ in a Vacuum Atmospheres inert-atmosphere glovebox. Solvents were reagent grade and were distilled from the appropriate drying agents under $N_2$ and degassed by the freeze–thaw method at least three times prior to use. $^1H$ NMR spectra were recorded on a Bruker AC-300 spectrometer operating at 300 MHz. Trace amounts of protonated solvents were used as reference, and chemical shifts are reported relative to $SiMe_4$. Combustion analyses were performed by Galbraith Laboratories Inc., Knoxville, TN, and Schwarzkopf Laboratories, Woodside, NY. MeLi and $Cp_2ZrCl_2$ were purchased from the Aldrich Chemical Co. $Cp_2ZrMe_2$ was prepared by the literature method.[6]

**Table I. Crystallographic Parameters**

| | complex 1 | complex 2 |
|---|---|---|
| formula | $C_{30}H_{58}O_4Zr_2$ | $C_{36}H_{36}O_4Zr_2$ |
| cryst color, form | colorless blocks | colorless blocks |
| $a$, Å | 8.585 (2) | 18.976 (4) |
| $c$, Å | 20.200 (2) | |
| $\alpha$, deg | | 117.99 (1) |
| cryst syst | tetragonal | trigonal |
| space group | $P4_2mnm$ | $R\bar{3}$ |
| vol, Å$^3$ | 1488.7 (5) | 2485.6 (8) |
| calcd density, g cm$^{-3}$ | 1.48 | 1.43 |
| $Z$ | 2 | 3 |
| cryst dimens, mm | 0.40 × 0.35 × 0.45 | 0.45 × 0.32 × 0.44 |
| abs coeff, $\mu$, cm$^{-1}$ | 6.40 | 5.79 |
| radiation λ, Å | Mo K$\alpha$ (0.71069) | Mo K$\alpha$ (0.71069) |
| temp, °C | 24 | 24 |
| scan speed, deg min$^{-1}$ | 4.0–10.0 ($\theta/2\theta$) | 2.0–5.0 ($\theta/2\theta$) |
| scan range, deg | 1.0 below K$\alpha_1$, 1.0 above K$\alpha_2$ | 1.0 below K$\alpha_1$, 1.0 above K$\alpha_2$ |
| bkgd/scan time ratio | 0.5 | 0.5 |
| no. of data collected | 587 | 2526 |
| $2\theta$ range, deg | 4.5–50 | 4.5–45.0 |
| index range | $+h,+k,+l$ | $\pm h,+k,+l$ |
| no. of unique data, $F_o^2 > 3\sigma(F_o^2)$ | 453 | 1411 |
| variables | 55 | 190 |
| $R$, % | 4.02 | 5.31 |
| $R_w$, % | 4.22 | 5.71 |
| largest $\Delta/\sigma$ in final least-squares cycle | 0.007 | 0.004 |
| max residual, e Å$^{-3}$ | 0.40 | 0.57 |
| atom associated | Zr | Zr |

**Synthesis of $Cp_2Zr(OCH_2C(CH_3)_2CH_2O)_2ZrCp_2$ (1).** A solution of 2,2-dimethylpropane-1,3-diol (0.042 g, 0.402 mmol) in 4 mL of THF was added to the solid $Cp_2ZrMe_2$ (0.100 g, 0.398 mmol), and the reaction mixture was allowed to stand for 8 h. Subsequent addition of 1–3 mL of hexane and further standing at 25 °C afforded a crystalline product. In some cases, this method yielded X-ray-quality, colorless crystals of the product 1 (yield 0.100 g, 65%). Anal. Calcd for $C_{30}H_{40}O_4Zr_2$: C, 55.69; H, 6.23. Found: C, 54.69; H, 6.23.[7] $^1H$ NMR (acetone-$d_6$, $\delta$ ppm): 6.37 (s, 20 H, Cp), 3.35 (s, 8 H, $CH_2$), 0.85 (s, 12 H, $CH_3$).

**Synthesis of $Cp_2Zr(m\text{-}OCH_2C_6H_4CH_2O)_2ZrCp_2$ (2).** 1,3-Benzenedimethanol (0.055 g, 0.400 mmol) and $Cp_2ZrMe_2$ (0.100 g, 0.398 mmol) were placed in a vial. To the vial was added 4 mL of THF. Methane evolution was readily apparent, and this continued for over 1 h. The reaction mixture was allowed to stand for 8 h. Subsequent addition of 1–3 mL of hexane and further standing at 25 °C afforded a milky solution and some of the crystalline product 2. The cloudy solution was decanted, affording the isolation of X-ray-quality, colorless crystals of the product (yield 0.040 g, 29%). Anal. Calcd for $C_{36}H_{36}O_4Zr_2$: C, 60.46; H, 5.07. Found: C, 60.04; H, 5.23. $^1H$ NMR (acetone-$d_6$, $\delta$, ppm):

(2) (a) The subject of early/late heterobimetallics has been recently reviewed: Stephan, D. W. *Coord. Chem. Rev.* **1989**, *95*, 41. Recent papers in the field include: (b) Wark, T. A.; Stephan, D. W. *Organometallics* **1989**, *8*, 2836. (c) Wark, T. A.; Stephan, D. W. *Inorg. Chem.*, in press. (d) Zheng, P. Y.; Nadasdi, T. T.; Stephan, D. W. *Organometallics* **1989**, *8*, 1393. (e) Dick, D. G.; Stephan, D. W. *Organometallics* **1990**, *9*, 1910. (f) Anderson, G. K.; Lin, M. *Organometallics* **1988**, *7*, 2285. (g) Ferguson, G. S.; Wolczanski, P. T.; Parkanyi, L.; Zonnvylle, M. C. *Organometallics* **1988**, *7*, 1967. (h) Darensbourg, M. Y.; Silva, R.; Reibenspies, J.; Prout, C. K. *Organometallics* **1989**, *8*, 1989.

(3) Early work in this area has been partially reviewed in: Malhotra, K. C.; Martin, R. L. *J. Organomet. Chem.* **1982**, *239*, 159.

(4) (a) Beshouri, S. M.; Fanwick, P. E.; Rothwell, I. P.; Huffman, J. C. *Organometallics* **1987**, *6*, 2498. (b) Durfee, L. D.; Latesky, S. L.; Rothwell, I. P.; Huffman, J. C.; Folting, K. *Inorg. Chem.* **1985**, *24*, 4569. (c) Chamberlain, L. R.; Keddington, J.; Rothwell, I. P. *Organometallics* **1982**, *1*, 1098. (d) Durfee, L. D.; Fanwick, P. E.; Rothwell, I. P.; Folting, K.; Huffman, J. C. *J. Am. Chem. Soc.* **1987**, *109*, 4720. (e) Chesnut, R. W.; Fanwick, P. E.; Rothwell, I. P. *Inorg. Chem.* **1988**, *27*, 752. (f) Chamberlain, L.; Rothwell, I. P.; Huffman, J. C. *J. Am. Chem. Soc.* **1986**, *106*, 1502. (g) Fanwick, P. E.; Ogilvy, A. E.; Rothwell, I. P. *Organometallics* **1987**, *6*, 73. (h) Chamberlain, L. R.; Rothwell, I. P. *J. Am. Chem. Soc.* **1983**, *105*, 1665. (i) Chamberlain, L. R.; Keddington, J.; Rothwell, I. P.; Huffman, J. C. *Organometallics* **1982**, *1*, 1538. (j) Steffey, B. D.; Chesnut, R. W.; Kerschner, J. L.; Pellechia, P. J.; Fanwick, P. E.; Rothwell, I. P. *J. Am. Chem. Soc.* **1989**, *111*, 378. (k) Chamberlain, L. R.; Rothwell, A. P.; Rothwell, I. P. *J. Am. Chem. Soc.* **1984**, *106*, 1847. (l) Coffindaffer, T. W.; Steffy, B. D.; Rothwell, I. P.; Folting, K.; Huffman, J. C.; Streib, W. E. *J. Am. Chem. Soc.* **1989**, *111*, 4742. (m) Steffy, B. D.; Chamberlain, L. R.; Chesnut, R. W.; Chebi, D. E.; Fanwick, P. E.; Rothwell, I. P. *Organometallics* **1989**, *8*, 1419. (n) Chamberlain, L. R.; Kerschner, J. L.; Rothwell, A. P.; Rothwell, I. P.; Huffman, J. C. *J. Am. Chem. Soc.* **1987**, *109*, 6471. (o) McMullen, A. K.; Rothwell, I. P.; Huffman, J. C. *J. Am. Chem. Soc.* **1985**, *107*, 1072. (p) Fanwick, P. E.; Kobriger, L. M.; McMullen, A. K.; Rothwell, I. P. *J. Am. Chem. Soc.* **1986**, *108*, 8095. (q) Latesky, S. L.; Keddington, J.; McMullen, A. K.; Rothwell, I. P.; Huffman, J. C. *Inorg. Chem.* **1985**, *24*, 995. (r) Latesky, S. L.; McMullen, A. K.; Niccolai, G. P.; Rothwell, I. P.; Huffman, J. C. *Organometallics* **1985**, *4*, 902. (s) Chamberlain, L. R.; Durfee, L. D.; Fanwick, P. E.; Kobriger, L. M.; Latesky, S. L.; McMullen, A. K.; Steffy, B. D.; Rothwell, I. P.; Folting, K.; Huffman, J. C. *J. Am. Chem. Soc.* **1987**, *109*, 6068. (t) Durfee, L. D.; McMullen, A. K.; Rothwell, I. P. *J. Am. Chem. Soc.* **1988**, *110*, 1463. (u) Latesky, S. L.; McMullen, A. K.; Niccolai, G. P.; Rothwell, I. P.; Huffman, J. C. *Organometallics* **1985**, *4*, 1896. (v) Latesky, S. L.; McMullen, A. K.; Rothwell, I. P.; Huffman, J. C. *J. Am. Chem. Soc.* **1985**, *107*, 5981. (w) Chamberlain, L. R.; Durfee, L. D.; Fanwick, P. E.; Kobriger, L. M.; Latesky, S. L.; McMullen, A. K.; Steffy, B. D.; Rothwell, I. P.; Folting, K.; Huffman, J. C.; Streib, W. E.; Wang, R. *J. Am. Chem. Soc.* **1987**, *109*, 390.

(5) (a) Lubben, T. V.; Wolczanski, P. T.; Van Duyne, G. D. *Organometallics* **1984**, *3*, 977. (b) La Pointe, R. E.; Wolczanski, P. T.; Mitchell, J. F. *J. Am. Chem. Soc.* **1986**, *108*, 6382. (c) La Pointe, R. E.; Wolczanski, P. T. *J. Am. Chem. Soc.* **1986**, *108*, 3535. (d) Toreki, R.; La Pointe, R. E.; Wolczanski, P. T. *J. Am. Chem. Soc.* **1987**, *109*, 7558. (e) La Pointe, R. E.; Wolczanski, P. T.; Van Duyne, G. D. *Organometallics* **1985**, *4*, 1810. (f) Neithamer, D. R.; La Pointe, R. E.; Wheeler, R. A.; Richeson, D. S.; Van Duyne, G. D.; Wolczanski, P. T. *J. Am. Chem. Soc.* **1989**, *111*, 9356.

(6) (a) Hunter, W. E.; Hrncir, D. C.; Vann Bynum, R.; Penttila, R. A.; Atwood, J. L. *Organometallics* **1983**, *2*, 750. (b) Samuel, E.; Rausch, M. D. *J. Am. Chem. Soc.* **1973**, *95*, 6263.

(7) Although several sets of X-ray-quality crystals of 1 were sent for analysis, the results were consistently off on carbon. Similar problems for early-metal chalogenide species have been previously described. (a) Shaver, A.; McCall, J. M. *Organometallics* **1984**, *3*, 1823. (b) Coutts, R. S.; Surtees, J. R.; Swan, J. R.; Wailes, P. C. *Aust. J. Chem.* **1966**, *19*, 1377. (c) Wark, T. A.; Stephan, D. W. *Inorg. Chem.* **1987**, *26*, 363. (d) White, G. S.; Stephan, D. W. *Organometallics* **1988**, *7*, 903.

**Table II. Positional Parameters (×10⁴)**

| atom | x | y | z | atom | x | y | z |
|---|---|---|---|---|---|---|---|
| | | | Complex 1 | | | | |
| Zr | 0 | 0 | 1460 (1) | O | 1239 (5) | 1239 (5) | 850 (3) |
| C1 | 7884 (9) | 2116 (9) | 1419 (6) | C2 | -2698 (8) | 815 (11) | 1832 (5) |
| C3 | -1865 (10) | 735 (9) | 2377 (4) | C4 | 1192 (14) | 2654 (13) | 441 (6) |
| C5 | 2643 (9) | 2643 (9) | 0 | C6 | 2616 (19) | 4117 (14) | 435 (6) |
| | | | Complex 2 | | | | |
| Zr | 3103 (1) | 3608 (1) | 58 (1) | O2 | 6230 (7) | 4917 (7) | -461 (7) |
| C1 | 929 (9) | 522 (9) | -3429 (9) | C2 | 5734 (13) | 3703 (13) | -1151 (14) |
| C11 | 1618 (9) | 511 (9) | -3600 (9) | C12 | 3250 (10) | 1988 (10) | -2392 (10) |
| C13 | 3919 (11) | 2020 (11) | -2529 (11) | C14 | 2884 (14) | 494 (14) | -3944 (13) |
| C15 | 1240 (13) | -1003 (12) | -5176 (12) | C16 | 594 (11) | -1017 (10) | -5026 (10) |
| C21 | 6026 (11) | 5552 (13) | 2129 (13) | C22 | 6320 (11) | 6446 (12) | 3143 (12) |
| C23 | 5534 (15) | 5588 (17) | 3011 (13) | C24 | 4746 (13) | 4138 (14) | 1892 (15) |
| C25 | 5105 (13) | 4190 (14) | 1420 (15) | C31 | 1719 (14) | 3339 (15) | 141 (15) |
| C32 | 743 (12) | 2520 (13) | -1264 (14) | C33 | -46 (11) | 1152 (13) | 2393 (13) |
| C34 | 362 (16) | 995 (15) | -1795 (20) | C35 | 1498 (20) | 2357 (26) | -138 (24) |
| O1 | 2168 (8) | 2066 (8) | -1815 (8) | | | | |

7.36, 7.25 (m, 8 H, Ph), 6.38 (s, 20 H, Cp), 4.63 (s, 8 H, $CH_2$).

**X-ray Data Collection and Reduction.** X-ray-quality crystals were obtained directly from the preparations as described above. The crystals were manipulated and mounted in capillaries in a glovebox, thus maintaining a dry, $O_2$-free environment for each of the crystals. Diffraction experiments were performed on a four-circle Syntex $P2_1$ diffractometer with graphite-monochromatized Mo K$\alpha$ radiation. The initial orientation matrices were obtained from 15 machine-centered reflections selected from rotation photographs. These data were used to determine the crystal systems. Partial rotation photographs around each axis were consistent with tetragonal and trigonal crystal systems for **1** and **2**, respectively. Ultimately, 50 and 34 reflections ($20° < 2\theta < 25°$) were used to obtain the final lattice parameters and the orientation matrices. Machine parameters, crystal data, and data collection parameters are summarized in Table I. The observed extinctions were consistent with the space groups $P4_2mnm$ and $R\bar{3}$ for **1** and **2**, respectively, and these groups were confirmed by the refinement. The data $hkl$ for **1** and $\pm h,+k,+l$ for **2** were collected in one shell ($4.5° < 2\theta < 45.0°$), and three standard reflections were recorded every 197 reflections. In the case of **1** an additional second shell of data ($45° < 2\theta < 50°$) was collected. The intensities of the standards showed no statistically significant change over the duration of the data collection. The data were processed with use of the SHELX-76 program package at the computing facilities of the University of Windsor. The reflections with $F_o^2 > 3\sigma(F_o^2)$ were used in the refinement.

**Structure Solution and Refinement.** Non-hydrogen atomic scattering factors were taken from the literature tabulations.[8] The Zr atom positions were determined by direct methods with use of SHELX-86. The remaining non-hydrogen atoms were located from successive difference Fourier map calculations. The refinements were carried out by using full-matrix least-squares techniques on $F$, minimizing the function $w(|F_o| - |F_c|)^2$, where the weight, $w$, is defined as $4F_o^2/2\sigma(F_o^2)$ and $F_o$ and $F_c$ are the observed and calculated structure factor amplitudes. In the final cycles of refinement all the non-hydrogen atoms were assigned anisotropic temperature factors. Hydrogen atom positions were calculated and allowed to ride on the carbon to which they are bonded, assuming a C–H bond length of 0.95 Å. Hydrogen atom temperature factors were fixed at 1.10 times the isotropic temperature factor of the carbon atom to which they are bonded. In all cases the hydrogen atom contributions were calculated but not refined. The final values of $R$ and $R_w$ are given in Table I. The maximum $\Delta/\sigma$ on any of the parameters in the final cycles of the refinement and the location of the largest peaks in the final difference Fourier map calculation are also given in Table I. The residual electron densities were of no chemical significance. The following data are tabulated: positional parameters (Table II) and selected bond distances and angles (Table III). Thermal parameters (Table S1), hydrogen atom parameters (Table S2), and values of $10F_o$ and $10F_c$ (Table S3) have been deposited as supplementary material.

**Table III. Selected Bond Distances (Å) and Angles (deg)**

| | | | | | |
|---|---|---|---|---|---|
| | | | Complex 1 | | |
| | | | Distances | | |
| Zr–O | 1.945 (6) | Zr–C1 | 2.570 (11) | Zr–C2 | 2.534 (7) |
| Zr–C3 | 2.528 (7) | O–C4 | 1.469 (11) | C4–C5 | 1.532 (12) |
| C4–C6 | 1.753 (18) | Zr···Zr | 5.898 | | |
| | | | Angles | | |
| O–ZrO′ | 101.4 (3) | | C4–O–Zr | 142.5 (5) | |
| C5–C4–O | 107.4 (7) | | C4–C5–C4′ | 110 (1) | |
| C6–C5–C6′ | 110 (1) | | | | |
| | | | Complex 2 | | |
| | | | Distances | | |
| Zr–O1 | 1.946 (6) | Zr–C21 | 2.558 (8) | Zr–C22 | 2.558 (8) |
| Zr–C23 | 2.550 (10) | Zr–C24 | 2.535 (11) | Zr–C25 | 2.549 (10) |
| Zr–C31 | 2.526 (8) | Zr–C32 | 2.554 (8) | Zr–C33 | 2.547 (8) |
| Zr–C34 | 2.502 (9) | Zr–C35 | 2.523 (10) | O1–C1 | 1.359 (9) |
| O2–C2 | 1.372 (10) | O1–C1 | 1.359 (9) | C1–C11 | 1.494 (10) |
| C2–C13 | 1.511 (12) | Zr···Zr | 6.833 | | |
| | | | Angles | | |
| O1–Zr–O2 | 99.4 (1) | | C1–O1–Zr | 155.1 (5) | |
| C11–C1–O1 | 113.3 (6) | | C13–C2–O2 | 113.5 (7) | |
| C12–C11–C1 | 121.7 (6) | | C16–C11–C1 | 120.6 (7) | |
| C12–C13–C2 | 120.4 (8) | | C14–C13–C2 | 121.5 (8) | |

**Molecular Modeling Considerations.** Energy minimization calculations were performed by employing the MMX and MM2 options of the program package PC-MODEL[9] operating on an IBM-PC-XT computer. Initial molecular coordinates were taken from the X-ray structural studies. The geometry about the metal centers was constrained to be that derived from the crystallographic data, as appropriate force fields are not available for Zr.

**Molecular Orbital Calculations.** These calculations and plotting were performed by employing the TRIBBL program package[9] operating on a VAX 11/785 computer. Extended Hückel calculations were performed by employing the EHT option of TRIBBL. Geometry optimizations were done by using the OPT9 routine. Cartesian coordinates of the various conformations of the model compound $Cp_2Zr(OH)_2$ were derived from the crystallographic data presented herein, with use of PC-MODEL.

## Results and Discussion

The reaction of metal alkyls with acidic proton sources leads to metal–carbon bond cleavage and formation of a metal–heteroatom bond. For example, reactions of

(8) (a) Cromer, D. T.; Mann, J. B. *Acta Crystallogr., Sect. A: Cryst. Phys., Diffr., Theor. Gen. Crystallogr.* **1968**, *A24*, 324. (b) Cromer, D. T.; Mann, J. B. *Acta Crystallogr., Sect. A: Cryst. Phys., Diffr., Theor. Gen. Crystallogr.* **1968**, *A24*, 390. (c) Cromer, D. T.; Waber, J. T. *International Tables for X-ray Crystallography*; Kynoch Press: Birmingham, England, 1974.

(9) Commercially available from Serena Software, Bloomington, IN.
(10) Pensak, D. A.; Wendoloski, J. J. Quantum Chemistry Program Exchange, Program No. 529.

**Scheme I**

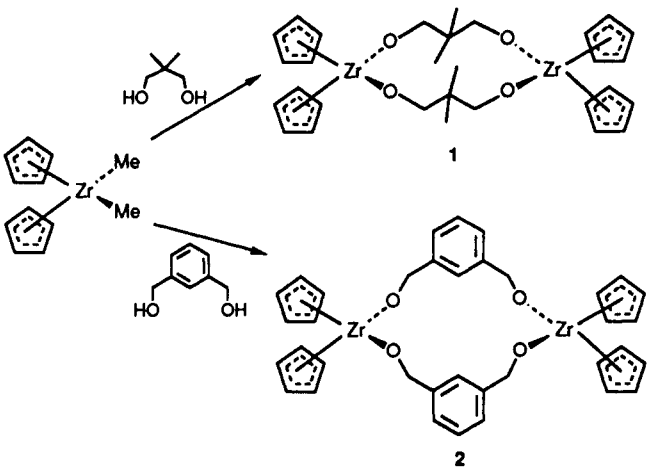


$Cp_2ZrMe_2$ with alcohols are known to proceed rapidly to liberate methane and form simple zirconium alkoxide species.[11,12] In this vein, addition of THF to a mixture of solid 2,2-dimethylpropane-1,3-diol and $Cp_2ZrMe_2$ results in the rapid liberation of methane. The resulting zirconium alkoxide species 1 crystallizes on standing or can be precipitated by addition of hexane. The isolated crystalline solid is only slightly soluble in THF, acetone, and $CDCl_3$. When it stands in these solvents, the compound decomposes. Although the nature of the degradation products is not known, hydrolysis by traces of water is implied by the acceleration of the degradation in "wet" solvents. The $^1H$ NMR spectrum of the product shows singlet resonances attributable to the presence of cyclopentadienyl, methylene, and methyl protons. No resonances attributable to Zr–Me fragments were observed. The integration of the $^1H$ NMR spectrum suggested the empirical formulation of 1 as $Cp_2Zr(OCH_2C(CH_3)_2CH_2O)$. A crystallographic study (vide infra) of 1 showed that it is, in fact, the dimer $[Cp_2Zr(\mu\text{-}OCH_2C(CH_3)_2CH_2O)]_2$.

In a similar manner, the reaction of $Cp_2ZrMe_2$ with 1,3-benzenedimethanol proceeds with the rapid evolution of methane. The colorless solution becomes cloudy white upon addition of hexane. When the solution stands, relatively low yields of crystalline product are obtained. The product 2 is isolated by decantation of the mother liquor, and the crystals are dried in vacuo. The $^1H$ NMR spectrum of 2 shows singlet resonances arising from the cyclopentadienyl and methylene protons and multiplets attributable to the phenyl protons. Again, the integration is consistent with a 1:1 combination of the $Cp_2Zr$ moiety and the dialkoxide. A crystallographic study confirmed that 2 is also a dimer, that is $[Cp_2Zr(\mu\text{-}OCH_2C_6H_4CH_2O)]_2$ (vide infra). The reactions are summarized in Scheme I.

**Structural Studies.** A crystallographic study showed that 1 crystallizes in the space group $P4_2mnm$ with two discrete dimeric molecules per unit cell. The Zr atom separation within the dimeric molecule is found to be 5.898 Å. The symmetry of the space group imposes 4 site symmetry on the molecule; thus, the asymmetric unit contains one-eighth of a dimer of 1. Symmetry operations on half of a cyclopentadienyl ring generate the two cyclopentdienyl rings that are $\pi$-bonded to each of the Zr centers. Symmetry-related oxygen atoms of the alkoxide moieties complete the pseudotetrahedral coordination spheres of the Zr atoms. The crystallographically imposed symmetry is

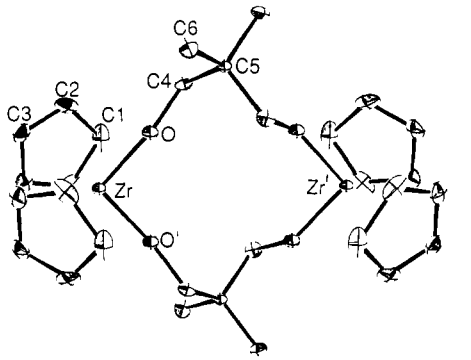


**Figure 1.** ORTEP drawing of molecule 1. Thermal ellipsoids at the 20% level are shown. Hydrogen atoms are omitted for clarity.

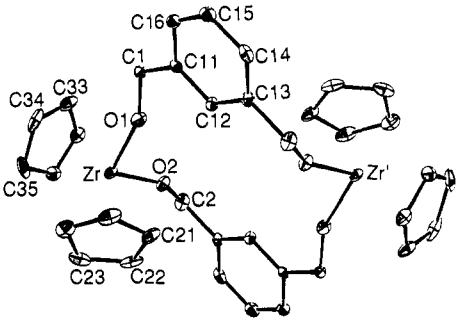


**Figure 2.** ORTEP drawing of molecule 2. Thermal ellipsoids at the 20% level are shown. Hydrogen atoms are omitted for clarity.

accommodated by a 50:50 disorder of the methylene and methyl fragments of the bridging dialkoxides that link the two Zr centers. Thus, for each dialkoxide moiety four methylene and four methyl carbon positions were refined. An ORTEP drawing of 1 showing one set of the disordered atoms appears in Figure 1.

The structural study of 2 showed that it crystallizes in the space group $R\bar{3}$ with three molecules in the unit cell. Again, the molecular formulation is confirmed as a dimer with a Zr...Zr distance of 6.833 Å. The site symmetry imposed on the molecule relates one half of the dimer to the other. As in 1, the pseudotetrahedral coordination sphere of Zr is completed by two $\pi$-bonded cyclopentadienyl rings and two bound oxygen atoms of the bridging dialkoxide ligands. An ORTEP drawing of 2 is shown in Figure 2.

Carbon–carbon bond distances and angles within the dialkoxide and cyclopentadienyl ligand fragments are as expected for both 1 and 2. The C–Zr distances for 1 and 2 average 2.544 (19) and 2.541 (13) Å, respectively, and are typical of $Cp_2Zr^{IV}$ derivatives.[2d-f] Selected bond distances and angles for the two structures are given in Table III.

The X–M–X angle at the metal center in bent metallocene derivatives depends on the electron configuration of the metal center. In the present complexes, the O–Zr–O angles were found to be 101.4 (3) and 99.4 (1)° in 1 and 2, respectively. These angles are comparable in magnitude to the S–Nb–S angle of 101.4 (1)° found in the $d^0$ species $[Cp_2Nb(SPh)_2][PF_6]$[2h] but are larger than the corresponding angles found for related $d^1$ species $(Cp_2V(SMe)_2$, 88.7 (1)°;[2b] $Cp_2NbCl_2$, 85.6 (1)°;[13] $[Cp_2MoCl_2]^+$, 82.0 (2)°;[13] $(MeC_5H_4)_2VCl_2$, 87.1 (1)°;[14] $Cp_2VS_5$, 89.3 (1)°;[15] $Cp_2V$-

(11) Chaudhari, M. A.; Stone, F. G. A. *J. Chem. Soc.* **1966**, 838.
(12) Babaian, E. A.; Hrncir, D. C.; Bott, S. G.; Atwood, J. L. *Inorg. Chem.* **1986**, *25*, 4818.
(13) Prout, K.; Cameron, T. S.; Forder, R. A.; Critchley, S. R.; Denton, B.; Ress, G. V. *Acta Crystallogr., Sect. B: Struct. Crystallogr. Cryst. Chem.* **1974**, *B30*, 2290.
(14) Petersen, J. L.; Dahl, L. F. *J. Am. Chem. Soc.* **1975**, *97*, 6422.
(15) Muller, E. G.; Petersen, J. L.; Dahl, L. F. *J. Organomet. Chem.* **1976**, *111*, 91.

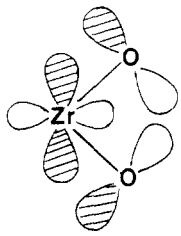


**Figure 3.** Schematic depiction of $d\pi$–$p\pi$ bonding in $Cp_2Zr(OH)_2$ derived from the $1a_1$ $Cp_2Zr$ fragment orbital and the oxygen p orbitals.

$(SPh)_2$, 94.1 (1)°;[16] $Cp_2Nb(SPh)_2$, 74.8 (1)°[3h]). Lauher and Hoffman[17] have explained the greater X–M–X angle in $d^0$ bent metallocene derivatives compared to that of the $d^1$ analogues in terms of the occupation of the $1a_1$ orbital. By extended Hückel methods the optimum O–Zr–O angle based on the minimization of the total energy was calculated for the model compound $Cp_2Zr(OH)_2$. The calculated energy minimum occurs when the O–Zr–O angle is 97.9°; however, little energy difference occurs over the angle range of 96–101°. This suggests that steric factors may account both for the discrepancies between the calculated angle and those observed and for the variation in the values seen in **1** and **2**.

The Zr–O distances were found to be 1.945 (6) Å in **1** and 1.939 (5) and 1.935 (5) Å in **2**. These distances are similar to those previously reported for zirconium peralkoxide species[4] and dramatically shorter than the Zr–S distances found for zirconocene thiolate derivatives (2.542 (2)–2.554 (2) Å[18]). The Zr–O bond distance is even shorter than expected on the basis of the difference in the covalent radii of oxygen and sulfur. This seems to implicate greater double-bond character in Zr–O bonds than in Zr–S bonds. The Zr–O–C angles of 142.5 (5)° found for **1** and 154.9 (4) and 152.8 (4)° found for **2** are less than the Zr–O–Si angle of 171 (1)° found for $(DME)ZrCl_2(OSiPh_3)_2$,[12] where Zr–O $\pi$ bonding has been implied. Similar early-metal–oxygen $\pi$ bonding has been implied in several other systems.[19-23]

The macrocyclic nature of the present complexes is reminiscent of that of crown ethers. The cavities within the rings are substantial, as indicated by the O...O distances (for **1**, 3.009, 3.434, 4.565 Å; for **2**, 2.954, 5.784, 4.964 Å). While one might consider the possibility of complexation studies, the structural data suggest that the donor ability of the oxygen atoms in the present complexes may be diminished by $\pi$ bonding to Zr. One might consider the incorporation of additional donor atoms by the use of $HO(CH_2)_xY(CH_2)_xOH$ or $HO(CH_2)_xY(CH_2)_xY(CH_2)_xOH$, where Y = O, S, N, or P, to enhance the ability of these macrocycles to bind other metals.

**Bonding Considerations.** To further investigate the nature of such $\pi$ bonding in **1** and **2**, we have performed extended Hückel molecular orbital calculations on the model $Cp_2Zr(OH)_2$. The results are consistent with those predicted on the basis of a frontier orbital picture for bent metallocenes, originally described by Hoffman and Lauher.[17] High-energy, unoccupied molecular orbitals with metal d orbital character are best described as those derived from the $a_2$ and $b_1$ frontier orbitals of the $Cp_2Zr$ fragment. Zr–O $\sigma$ bonding is derived primarily from the $2a_1$ and $b_2$ frontier orbitals, while the HOMO is largely $1a_1$ in character. In addition, the $a_1$ metal fragment orbitals are of correct symmetry to stabilize the p orbitals on the oxygen atoms. This mixing is depicted in Figure 3. This interaction is reminiscent of that described for $Cp_2Ti(CO)_2$, where the occupied $1a_1$ orbital is stabilized by mixing with the $\pi^*$ orbitals of CO.[17] Of course, the symmetry of the orbital interactions is similar in these cases; in $Cp_2Zr(OH)_2$ the MO is derived from occupied ligand orbitals and a vacant metal fragment orbital, while the reverse is true in the $d^2$ compound $Cp_2Ti(CO)_2$. In related calculations for $Cp_2Zr(SH)_2$, such $d\pi$–$p\pi$ mixing occurs to a much lesser extent, as expected on the basis of intuitive hard/soft analogies for metal–ligand bonding. Presumably the larger covalent radius of sulfur, as well as the poorer match in orbital energies between Zr and sulfur relative to that of oxygen, minimizes such mixing of the $1a_1$ metal fragment orbital with the p orbitals on sulfur, thus reducing the $\pi$ character in the M–S bond. This is reflected in the Zr–S bond distances.

**Conformational Considerations.** The disorder in the structural data for **1** is consistent with either a pseudocrown (**1a**) or a pseudochair (**1b**) conformer. The cyclopentadienyl groups are magnetically equivalent in the pseudocrown conformer, while for the pseudochair conformer the cyclopentadienyl moieties are inequivalent. The observation of a single resonance in the solution $^1H$ NMR spectrum of **1** suggests but does not confirm the presence of the pseudocrown conformer.

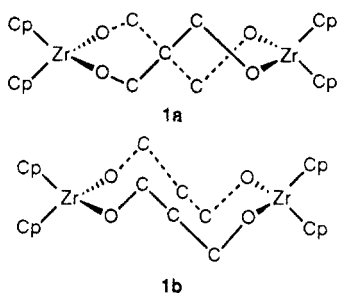


**1a**




**1b**

Further support of the thermodynamic preference for the pseudocrown conformer is derived from molecular modeling considerations. Initial molecular geometries for the two conformers were derived from the crystallographic data. Molecular mechanics calculations were performed with use of these two conformations as the starting points. The geometries about Zr were fixed, and the bonding was approximated as $Cp^-$ and $Zr{=}O^+{-}R$. Energy minimizations converged for each conformation with relatively little movement of the organic fragments, suggesting that both the pseudocrown and pseudochair conformations are energy minima for the macrocyclic rings. However, the total energy of the pseudocrown conformer is 19 kcal/mol lower than that of the pseudochair conformer. Variable-temperature $^1H$ NMR studies of **1** in acetone-$d_6$ between −50 and +50 °C showed no evidence of conformational fluxionality. The calculated energy difference between the conformers may be overestimated, as the calculations exclude energy terms involving the metal-containing fragment. However, the qualitative prediction of an energetic preference for the pseudocrown conformer is realistic, as significant alterations of the Zr geometry are not expected

(16) Muller, E. G.; Petersen, J. L.; Dahl, L. F. *J. Organomet. Chem.* **1976**, *111*, 73.
(17) Lauher, J. W.; Hoffmann, R. *J. Am. Chem. Soc.* **1976**, *98*, 1729.
(18) Petersen, J. L. *J. Organomet. Chem.* **1979**, *166*, 179.
(19) Huffman, J. C.; Moloy, K. G.; Marsella, J. A.; Caulton, K. G. *J. Am. Chem. Soc.* **1980**, *102*, 3009.
(20) Casey, C. P.; Jordan, R. F.; Rheingold, A. L. *J. Am. Chem. Soc.* **1983**, *105*, 665.
(21) Reger, D. L.; Tarquini, M. E.; Lebioda, L. *Organometallics* **1983**, *2*, 1763.
(22) Lubben, T. V.; Wolczanski, P. T.; Van Duyne, G. D. *Organometallics* **1984**, *3*, 977.
(23) Hunter, W. E.; Hrncir, D. C.; Bynum, R. V.; Pentilla, R. A.; Atwood, J. L. *Organometallics* **1983**, *2*, 750.

to accompany changes in the ring conformation.

The conformation of the dimetalated macrocycle **2** is best described as a pseudochair (**2a**). The differing con-

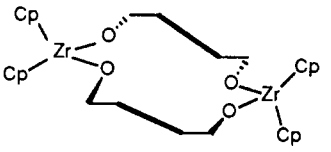

**2a**

formations of the macrocyclic rings for **1** and **2** result from the differing disposition of the substituents on oxygens. In the pseudocrown conformation of **1**, the C–O–Zr–O dihedral angles are 81.69° and thus the orientation of the alkyl substituent on the oxygen atoms is best described as endo (**3**). In **2**, the corresponding dihedral angles are

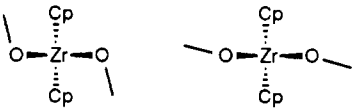

**3** **4**

121.84 and −164.78°; thus, the substituents are exo (**4**). Presumably, the pseudocrown conformation for **1** minimizes the steric interactions between endo substituents, whereas for **2** such steric interactions are avoided by the exo disposition of the ligands, and thus a pseudochair conformation is adopted. In a similar manner, the exo substituents in $[Cp_2Ti(C_8N_2O_8)ZrCp_2]_2$ and $[Cp_2Ti(C_8N_2O_8)TiCp_2]_2$ afford pseudochair conformations for the macrocyclic ring within these compounds.[24]

Molecular orbital and modeling calculations provide some insight into the question of substituent disposition. By extended Hückel methods, the total energy for $Cp_2Zr(OH)_2$ was calculated as a function of the H–O–Zr–O dihedral angles. The minimum total energy corresponded to dihedral angles of 85°. This endo orientation appears to be a compromise between the maximization of the $\pi$ interaction between the oxygen and the metal and the minimization of lone-pair–lone-pair repulsion. Molecular mechanics calculations also predict the energetic preference for the endo conformer of $Cp_2Zr(OH)_2$. In contrast, MMX calculations for $Cp_2Zr(OCH_3)_2$ predict that the exo conformer is energetically preferred. These results imply that steric demands may override the electronic preference for an endo conformation. Although these calculations may not accurately reflect the threshold for domination of ligand disposition by steric factors, the correlation between orientation and substituent size is consistent with literature data. For example, the methyl groups of $Cp_2M(SMe)_2$ (M = Ti, V)[2b] are endo, while the phenyl rings in $Cp_2Nb(SPh)_2$[2h] are exo in disposition. In addition, the observation of an endo conformation of the substituents in **1** and an exo disposition in **2** is consistent with the predicted size/orientation correlation.

**Acknowledgment.** Financial support from the NSERC of Canada is gratefully acknowledged.

**Supplementary Material Available:** Tables of thermal and hydrogen atom parameters and bond distances and angles (3 pages); a listing of values of $10F_o$ and $10F_c$ (8 pages). Ordering information is given on any current masthead page.

(24) Guthner, T.; Thewalt, U. *J. Organomet. Chem.* **1989**, *371*, 43.

# Heterometallic Analogues of $[(\eta^5\text{-}C_5Me_5)M(CO)_2]_2$ (M = Fe, Ru, Os). Synthesis and Structures of $(\eta^5\text{-}C_5Me_5)_2(CO)_4IrRe$, $(\eta^5\text{-}C_5Me_5)_2(CO)_4IrMn$, and $(\eta^5\text{-}C_5Me_5)(\eta^5\text{-}C_5H_5)(CO)_4IrRe$

Jun-Ming Zhuang, Raymond J. Batchelor, Frederick W. B. Einstein,* Richard H. Jones, Ramzi Hader, and Derek Sutton*

*Department of Chemistry, Simon Fraser University, Burnaby, British Columbia, Canada V5A 1S6*

*Received March 13, 1990*

The heterobimetallic, metal–metal bonded complexes $(\eta^5\text{-}C_5Me_5)(CO)Ir(\mu_2\text{-}CO)_2Mn(CO)(\eta^5\text{-}C_5Me_5)$ (**1**), $(\eta^5\text{-}C_5Me_5)(CO)Ir(\mu_2\text{-}CO)_2Re(CO)(\eta^5\text{-}C_5Me_5)$ (**2**), and $(\eta^5\text{-}C_5Me_5)(CO)Ir(\mu_2\text{-}CO)_2Re(CO)(\eta^5\text{-}C_5H_5)$ (**3**) have been synthesized by reaction of $(\eta^5\text{-}C_5R_5)M(CO)_2(THF)$ (M = Mn, R = H; M = Re, R = H, Me) with $(\eta^5\text{-}C_5Me_5)Ir(CO)_2$. The IR, NMR, and mass spectral data for these complexes are reported and are discussed in relation to the molecular structure of **3**, which has been established by X-ray diffraction. Crystals of **3** are orthorhombic, space group $Pna2_1$ with $a$ = 16.739 (2) Å, $b$ = 9.591 (2) Å, $c$ = 11.554 (2) Å, $V$ = 1854.9 Å$^3$, and $Z$ = 4. The structure has been refined to $R(F)$ = 0.027 from 1427 independent observed intensities with $I_o \geq 2.5\sigma(I_o)$ in the range $4° \leq 2\theta \leq 52°$. The $\eta^5\text{-}C_5Me_5$ with $\eta^5\text{-}C_5H_5$ groups are oriented trans as are the two terminal CO groups. The remaining two semibridging carbonyl groups are primarily bound to the Re atom. The Ir–Re bond length, not corrected for the thermal motion, is 2.8081 (6) Å.

## Introduction

The homometallic complexes $[Cp^*M(CO)_2]_2$ (M = Fe, Ru, Os; $Cp^* = \eta^5\text{-}C_5Me_5$)[1-3] have all been synthesized in recent years and may be compared with the earlier and generally better known cyclopentadienyl analogues $[CpM(CO)_2]_2$ ($Cp = \eta^5\text{-}C_5H_5$). To date, the osmium compound[3] has scarcely been studied; however, the ruthenium compound, like its Cp analogue, appears potentially to be a rich source of novel transformations at the diruthenium center.[4] Currently, there is considerable interest in heterobimetallic complexes,[5-7] stimulated in part by the an-

(1) King, R. B.; Efraty, A. *J. Am. Chem. Soc.* **1971**, *93*, 4950.
(2) King, R. B.; Iqbal, M. Z.; King, A. D., Jr. *J. Organomet. Chem.* **1979**, *171*, 53.
(3) (a) Weber, L.; Bungardt, D. *J. Organomet. Chem.* **1986**, *311*, 269. (b) Hoyano, J. K.; May, C. J.; Graham, W. A. G. *Inorg. Chem.* **1982**, *21*, 3095.

(4) Forrow, N. J.; Knox, S. A. R. *J. Chem. Soc., Chem. Commun.* **1984**, 679.

0276-7333/90/2309-2723$02.50/0 